Journal of Magnetism and Magnetic Materials 349 (2014) 144–148

Contents lists available at ScienceDirect

Journal of Magnetism and Magnetic Materials

journal homepage: www.elsevier.com/locate/jmmm

First-principles study of antisite defects effect on electronic and magnetic properties of $Mn_{2+x}Co_{1-x}Ga$

X.F. Zhu*, Y.X. Wang, L.F. Chen

Department of Physics, Nanjing Normal University, Nanjing 210097, China

ARTICLE INFO

Article history:
Received 20 October 2012
Received in revised form
6 June 2013
Available online 31 August 2013

Keywords:
Half-metal
First-principle
Electronic structure
Spin–orbit coupling
Magnetic property

ABSTRACT

The electronic structures and magnetic properties are reported for $Mn_{2+x}Co_{1-x}Ga$ (x=0.0, 0.25, 0.5) and $Mn_{2.25}Co_{0.75}Ga$ with antisite defects (AS) using first-principles density functional theory within the generalized gradient approximation (GGA) schemes. Electronic band structure calculations indicate that the perfect Mn_2CoGa is half-metallic and the half-metallic character is preserved for x=0.25 and x=0.5. AS defects of type(i) can maintain the half-metallic while AS defects of type(ii) are found to destroy the half-metallic and show metallic behavior. Based on the magnetic property calculations, the experimentally observed reduction of the magnetic moment mainly arises from weaker magnetic interactions of Mn and Co for higher Mn concentrations and the magnetic interactions are further weakening in the AS defect models.

1. Introduction

Half-metallic, which has a metallic band structure for one spin channel and an insulating band gap at the Fermi level for the opposite spin, thus providing a complete spin polarization of conducting electrons, has attracted more and more attentions because of its potential applications in spin-based electronic devices. The half-metallic has been found in many materials, for example in ferromagnetic metallic oxides, Heusler compounds, dilute magnetic semiconductors, binary transition-metal pnictides and chalcogenides with zinc-blende structure, etc. since its first discovery by de Groot et al. [1–6]. Among them, half-metallic Heusler alloys are expected to play a key role in realistic applications due to their very high Curie temperatures and their structural similarity to the widely used binary semiconductors crystallizing in the zinc-blende structure. For applications in spin transfer torque devices, a small magnetization combined with high spin polarization would considerably enhance the effective torque induced by a spin polarized current [7,8].

Heusler alloys are represented in general by the generic formula X_2YZ, where X and Y denote some transition-metal elements and Z an s–p element. Usually, the ternary compounds have a highly ordered $L2_1$ structure, which belongs to the $Fm\bar{3}m$ space group. However, ferrimagnets with large local moments and half-metallic properties have recently been predicted for compounds that form the $CuHg_2Ti$-type structure [9]. Its space group is $F\bar{4}3m$, the same as that of the semi-Heusler alloy. This crystal structure is based on a cubic structure with four interpenetrating fcc sublattices A, B, C, and D (Fig. 1). In ordered Mn_2CoGa the Mn atoms occupy the A and B sublattices; Co and Ga the C and D, respectively. In this structure two Mn atoms are in nearest neighbor positions to each other invoking an antiparallel alignment of their magnetic moments. It is shown that one of the two Mn moments has local character, whereas the other Mn moment and the Co moment are itinerant. It is the hybridization between the Mn(A) and Co atom that dominates the magnitude of magnetic moment of the Co atom and the sign of the Mn(B)–Co exchange interaction [9–11]. Therefore, we believe that it is the special crystallized structure that leads to a quite complex magnetic interaction and bring about many physical properties for the Mn_2Co-based alloys.

We investigate a series of $Mn_{2+x}Co_{1-x}Ga$ (x=0, 0.25, 0.5) compounds where the Co atom on the C site is successively substituted by Mn, tuning the magnetization to smaller values. For $0 < x < 0.3$, the Mn moments in experiment are much smaller than values calculated by first-principles calculation which may indicate a residual antisite (AS) defects in $Mn_{2+x}Co_{1-x}Ga$. We study the AS disorder between the Mn(B) and Co(C) superlattices at x=0.25 because it is easer to indicate disorder with MnCCo antisite defects at this concentration [12]. The theoretical calculations have shown that antisite disorder of a few percent in $Mn_{2+x}Co_{1-x}Ga$ can destroy half metallicity, emphasizing the importance of characterizing samples for disorder. The partial replacement of Co by Mn ($x > 0.3$) also avoids an occupation of B sites by Co at high Co concentrations, which would lead to a rapid degradation of the half-metallic properties.

2. Computational details

First-principles calculations of $Mn_{2+x}Co_{1-x}Ga$ are performed in a plane-wave basis set using the projector augmented wave (PAW) [13,14] method in the generalized gradient approximation (GGA)

* Corresponding author. Tel.: +86 25 84372962.
E-mail address: zxf_physics@163.com (X.F. Zhu).

0304-8853/$ - see front matter © 2013 Elsevier B.V. All rights reserved.
http://dx.doi.org/10.1016/j.jmmm.2013.08.051

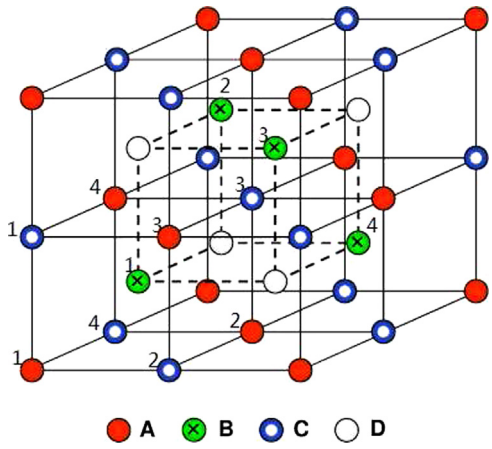

Fig. 1. The generalized cubic structure with four interpenetrating fcc sublattices A, B, C, and D. $Mn_{2+x}Co_{1-x}Ga$ crystallizes in the $CuHg_2Ti$-type structure with Mn occupying the A and B sublattices, Co the C site and Ga the D site.

as it is implemented in the Vienna *ab initio* simulation program (VASP) [15,16] program. A plane-wave basis and projector augmented-wave pseudopotentials are used, with Mn *d*6*s*, Co *d*8*s*1 and Ga *s*2*p*1 electrons treated selfconsistently. A 350 eV plane-wave cutoff results in good convergence of the total energies. Forces on atoms were calculated, and atoms were allowed to relax using a conjugate gradient technique until their residual forces had converged to less than 0.01 eV/Å. The Brillouin zone integration is performed using Monkhorst–Pack grids of $6\times6\times6$ during the iterations; but, to obtain higher quality state densities and to check the stability of the results, this number of k-points was increased to $10\times10\times10$ after convergence was reached.

The structural optimizations were performed for the 16-atom cell, which corresponds to a cubic unit cell consisting of four formula units (Fig. 1). It can be imagined as four interpenetrating face-centered-cubic (fcc) lattices with the basis vectors A=(0, 0, 0), B=(1/4, 1/4, 1/4), C=(1/2, 1/2, 1/2), and D=(3/4, 3/4, 3/4). In the ideal $x=0$ composition (the ordered Mn_2CoGa), the Mn occupies the nonequivalent A and B sites as nearest neighbors, Co resides on the C site and Ga is on the D site. For $x=0.25$ and $x=0.5$ we replace one and two Co atoms with Mn on C sites, respectively. In particular, according to experiments, the most likely antisite defects are: (i) Mn(A) antisites where interchanging the Mn(A) and Co sites, (ii) Mn(B) antisites where interchanging the Mn(B) and Co sites in our antisite defects calculations for $x=0.25$. In order to understand the magnetic properties of doped and antisite defects in $Mn_{2+x}Co_{1-x}Ga$, the A and B sites Mn and Co are designated as Mn1(A), Mn2(A), Mn3(A), and Mn4(A) and Mn1(B), Mn2(B), Mn3(B), and Mn4(B) and Co1, Co2, Co3, Co4 (labeled in Fig. 1). In the calculations involving spin–orbit coupling, it was included in scalar relativistic form as a perturbation to the original Hamiltonian.

3. Results and discussion

We show our calculated relaxed structural parameters for different compositions by using GGA methods in Table 1. The lattice parameters of Mn_2CoGa obtained experimentally are $a=b=c=$ 5.8620 Å. The unit cell shape, lattice vectors, and atomic coordinates were optimized simultaneously during optimizing. The unit cell volume almost unchanged when the Mn concentration increases which is probably due to the nearly same sizes of Mn and Co ions. The crystal structure of the compounds for $x=0.0$ and $x=0.25$ has a cubic lattice while the crystal structure of the compounds for $x=0.5$ has a tetragonal phase which are in good

Table 1
Calculated structural parameters and total magnetic moments for $Mn_{2+x}Co_{1-x}Ga$.

x	0.0	0.25	0.5
a (Å)	5.680	5.681	5.688
b (Å)	5.680	5.681	5.688
c (Å)	5.680	5.681	5.666
μ_T (μ_B/f.u.)	2.03	1.52	1.04

agreement with the experimental results [12]. The calculated total magnetic moments for $Mn_{2+x}Co_{1-x}Ga$ are also listed in Table 1. We notice that the total magnetic moments decrease with x and find a good agreement of the total magnetization determined by the sum rules. The calculated magnetic moments of Mn and Co are listed in Table 2 using GGA and GGA+SO methods. We stress that the moment per atomic sphere depends on the choice of the sphere radius. Since the latter is not uniquely defined, neither is the magnetic moment per sphere. Thus, a comparison of these numbers with equivalent numbers of other calculations or even with experimental ones is not necessarily very meaningful. Mn on the A site (Mn(A)) has a predicted magnetic moment of $-1.29\ \mu_B$, antiparallel to both its B site moment of $+2.52\ \mu_B$ and the Co moment of $+0.81\ \mu_B$ in Mn_2CoGa. Disentangling contributions of Mn atoms on different sublattices reveals fairly large antiparallel oriented Mn moments although the average magnetization is small. The two site Mn atoms are nearest neighbors to each other and exhibit different magnetic characters. Therefore, we believe that it is the special crystallized structure that leads to a quite complex magnetic interaction. In the $Mn_{2+x}Co_{1-x}Ga$, where the Co atom on the C site is substituted by Mn, the absolute magnetic moments of Mn2(A) are not the same as the other Mn(A) any more, which is strongly influenced by the next nearest-neighbor shell while the magnetic moments of Mn(B) decrease as the change of the nearest-neighbor shell. The absolute magnetic moments of Mn at C sites and Co decrease from $x=0.0$ to $x=0.5$ in Table 2 which may be weakened by a modulation of the Mn–Mn–Mn(Co) or Mn–Co–Ga bond angles, a realization of the so-called magnetic Jahn–Teller effect. The Mn(B) atom carries the largest moment in all the $Mn_{2+x}Co_{1-x}Ga$ compounds, which is similar to most of the Mn-based Heusler alloys. Usually, we think that the larger the magnetic moment, the stronger the exchange interaction. So, it is considered that the stronger the Mn(B)–Co and Mn(B)–Mn(A) exchange interaction is. The Mn(C) and Mn(A) have same signs while the Mn(C) and Mn(B) have opposite signs, i.e. the coupling between the C and A site Mn is ferromagnetic whereas within the B site is antiferromagnetic, which are different from C site Co. In order to explore the effect of spin–orbit coupling, we carried out GGA+SO calculations with the magnetization axis chosen along [001] direction. The orbital moment at the Co site turned out to be $0.03\ \mu_B$ with the orbital moment pointing along the direction of the spin moment in Mn_2CoGa. The orbital moment at the Mn site is tiny due to the t_{2g} configuration with no orbital degrees of freedom left and the direction of the orbital moment is different due to the Mn on different sites.

The spin-polarized GGA calculations, as shown in Fig. 2, give a half-metallic ground state with a finite density of states in the spin-up channel and a zero density of states in the spin-down channel crossing Fermi level from $x=0.0$ to $x=0.5$ in $Mn_{2+x}Co_{1-x}Ga$. From the total density of states (DOS), the lowest valence bands are separated from the other valence bands by an energy gap for both majority and minority spins and unaffected. For the majority-spin states, there appear to be three peaks. The two peaks at the lower energies can be traced to the e_g-t_{2g} splitting in the cubic crystal field, and the peak at the higher energy is composed of antibonding *d* bands of mostly Mn(A) character. For the minority-spin